PCCP

ROYAL SOCIETY OF CHEMISTRY

PAPER

View Article Online
View Journal

Cite this: DOI: 10.1039/d5cp00848d

Revealing formic acid adsorption geometries on magnetite (001) and (111) surfaces by IRRAS line shape analysis

Heshmat Noei, *[a] Marcus Creutzburg,[a] Gregor Vonbun-Feldbauer [bcd] and Andreas Stierle [ae]

Received 4th March 2025,
Accepted 23rd April 2026

DOI: 10.1039/d5cp00848d

rsc.li/pccp

The sign and intensity of infrared (IR) bands on oxide surfaces strongly depend on light polarization and the adsorption geometry of surface species. In this study, we investigate formic acid adsorption on single crystalline magnetite Fe_3O_4(001) and Fe_3O_4(111) surfaces, which being neither perfect metals nor insulators exhibit characteristic Fano shaped IR line profiles. Using both s- and p-polarized infrared reflection absorption spectroscopy (IRRAS), we identify distinct spectral features and reveal vibrational bands that were previously unobserved in experiments employing unpolarized or solely p-polarized light. Complementary density functional theory (DFT) calculations provide structural and vibrational insights into the adsorbed species. On Fe_3O_4(001), a new band at 1555 cm^{-1} observed with p-polarized light is attributed to the asymmetric OCO stretching vibration of formate bound to octahedral Fe sites with tetrahedral Fe_{tet1} underneath. On Fe_3O_4(111), a band at 1730 cm^{-1} detected in both unpolarized and s-polarized light corresponds to the C═O stretch of a monodentate species. These results highlight the crucial role of light polarization in IRRAS for elucidating adsorption geometries and electronic properties of oxide surfaces.

Introduction

In heterogeneous catalysis, infrared (IR) spectroscopy has been widely used in three main areas. The most common application is the identification and characterization of functional groups and organic compounds. It can also be used to determine the chemical states of catalysts *in situ* during chemical reactions. Another major application of IR spectroscopy is monitoring adsorbed molecules to gain insight into their geometry and adsorption type, which provides essential information about surface active sites and the electronic properties of substrates and catalysts.[1,2] Over the past decade, Fourier Transform Infrared Reflection Absorption Spectroscopy (FT-IRRAS) has undergone significant technological advancements. One of the most notable breakthroughs is the capability to perform high-sensitivity measurements on oxide single crystals. These developments have greatly enhanced the analytical power of infrared spectroscopy, particularly in surface science and the study of catalytic processes.

Modern state-of-the-art FT-IR spectrometers now offer a high signal-to-noise ratio, high resolution, rapid spectrum acquisition, and a wide scan range.[3,4] It has been shown that by combining an IR spectrometer with an ultra-high vacuum (UHV) chamber and a fully evacuated IR beam path, one can measure both powder and single crystalline surfaces in transmission and reflection modes, respectively; bridging the gap between ordered and non-ordered materials.[5–7]

Infrared reflection–absorption spectroscopy is an essential technique for studying adsorbed molecules on reflective surfaces. When an electromagnetic wave is reflected from a metal surface the s-polarized component of light which is polarized perpendicular to the plane of incidence undergoes a phase change of 180° independent of the incidence angle. This results in destructive interference and a zero electric field at the metal surface.

While metal single crystals completely absorb s-polarized light due to the surface selection rule, this restriction does not apply to oxides and dielectrics, which reflect both s- and p-polarized components. As a result, IR bands on these surfaces can display a mix of positive and negative line shapes. This characteristic, combined with the technical challenges of designing optical setups that can effectively distinguish between s- and p-polarized beams, has historically limited the development of IRRAS studies

[a] Deutsches Elektronen-Synchrotron DESY, Center of X-ray and Nano Science (CXNS), Notkestr. 85, 22607 Hamburg, Germany. E-mail: heshmat.noei@desy.de
[b] Hamburg University of Technology (TUHH), Institute for Interface Physics and Engineering, Am Irrgarten 3-9, 21073 Hamburg, Germany
[c] Hamburg University of Technology (TUHH), Institute of Advanced Ceramics, Denickestr. 15, 21073 Hamburg, Germany
[d] Helmholtz-Zentrum Hereon, Institute of Surface Science, Max-Planck-Str. 1, 21502 Geesthacht, Germany
[e] University of Hamburg, Department of Physics, Luruper Chaussee 149, 22607 Hamburg, Germany

on oxide surfaces. The s- and p-polarized components of light in IRRAS exhibit the position of an IR vibrational band that is characteristic of a specific functional group. They also reveal the shape and sign of the IR band, providing information about the dipole orientation and, ultimately, the geometry of an adsorbed feature on the surface of an oxide substrate.

In this paper we focus on the adsorption of formic acid (HCOOH), which has been studied extensively using IRRAS due to its important role in surface chemistry, catalysis, and environmental science.[8–12] The key reasons for studying formic acid adsorption are: (1) HCOOH readily adsorbs onto oxide surfaces, and state-of-the-art IRRAS is particularly well-suited for studying adsorption phenomena; (2) the adsorption of formic acid on oxide surfaces can occur *via* different modes, such as carboxylate COO, *i.e.* formate, as well as undissociated adsorption of the molecule. IRRAS can distinguish between these different modes by analyzing the vibration frequencies of specific bonds, which guide us to understand the interaction mechanisms between formic acid and the surface, providing insights into adsorption strength, molecular orientation, and bonding nature; (3) formic acid is often used as a probe molecule in surface catalysis studies, particularly in water–gas shift, CO oxidation and hydrogenation reactions. It helps to obtain information about the formation of intermediates, which are crucial for understanding the reaction mechanisms; (4) Last but not least, formic acid has been used to probe surface properties, because the adsorption of formic acid can be influenced by the type of oxides, surface defects, hydroxylation, and the presence of different metal cations. Furthermore, the surface chemistry of HCOOH on oxides is sensitive to the change in the dielectric property of the oxides, where the electronic nature of the substrate influences the strength of the coupling with the formic acid vibrational states. This phenomenon leads to an asymmetric line shape in the observed spectra known as Fano shaped line and provides another view of molecule-surface interactions, which is valuable for both fundamental research and applications in catalysis.

Fig. 1 illustrates the possible binding modes of formate on an oxide surface. These modes can vary depending on the substrate, coverage, and temperature. In the bidentate bridging mode, formate binds through both oxygen atoms to two metal atoms. If the metal atoms are too far apart, other configurations may form. In the bidentate chelating mode, both oxygens bind to the same metal atom. Monodentate adsorption involves only one oxygen binding to the surface. In quasi-bidentate geometry, one oxygen binds to a metal atom while the other binds to a surface hydroxyl group. Undissociated formic acid can also adsorb molecularly, with bonding delocalized over the carboxylic group.

Theoretical background: reflectivity and Fano line shape

The IRRAS spectra arise from the interaction of the vibrational transition dipole moment (TDM) with the electric field components of the incident light. Depending on the orientation of the adsorbed species and the polarization of light (s or p), different components of the dipole moment contribute to the absorption. For example, vibrational modes with a dipole moment component perpendicular to the surface couple strongly to p-polarized light, which contains a electric field component in the surface normal direction. This underlies the appearance and intensity of features in the IR spectra.

To understand the shape and sign of IR bands, it is essential to consider the components of the electric field in the incident IR beam, as illustrated in Fig. 2. The component that is parallel to the surface and perpendicular to the plane of incidence is referred to as s-polarized (E_s). In contrast, p-polarized light, confined to the plane of incidence and perpendicular to the beam, comprises two components: one parallel to the surface (tangential p-polarized, E_{pt}) and one perpendicular to it (normal p-polarized, E_{pn}). Only E_{pn}

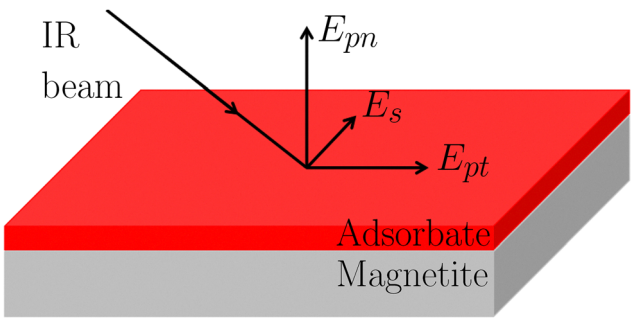

Fig. 2 Different electric field components in IRRAS: E_s and E_{pt} are parallel to the surface, E_{pn} is perpendicular to the surface. Layer 1 denotes vacuum ($\hat{n}_1 = 1 + 0i$), layer 2 is the adsorbate, layer 3 is the magnetite substrate.

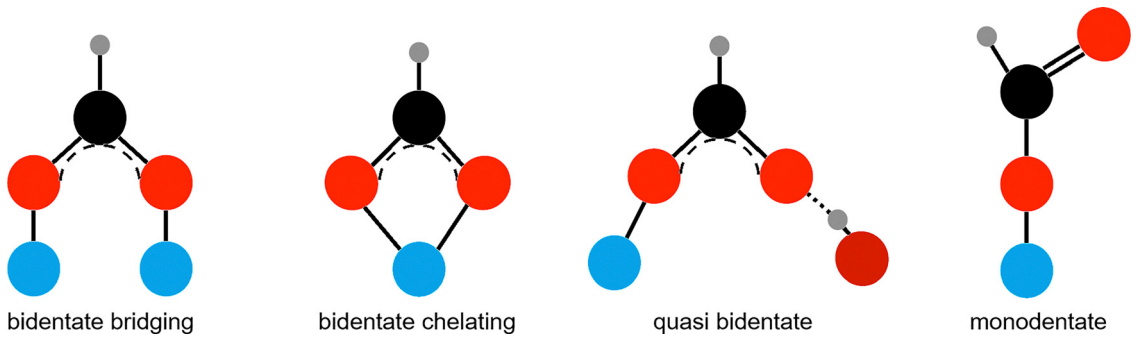

Fig. 1 Schematic drawing of possible binding geometries of formate species on metal oxides. The metal substrate atoms are shown in blue, formate oxygen in red, substrate oxygen in dark red, carbon in black and hydrogen in grey.

can excite molecular vibrations oriented normal to the surface (see Fig. 2), while vibrations aligned parallel to the surface can be excited by E_s and/or E_{pt}.[10,13,14]

The reflectivity differences, ΔR_i, which are calculated by subtracting the reflectivity of the surface after adsorption, R_i, from that of the clean surface, R_i^0, for each component i = {s, pt, pn} are plotted in Fig. 3 for HCOOH adsorption on magnetite.[13–18] Three main observations can be made. First, depending on the incidence angle θ, both ΔR_{pt} and ΔR_{pn} can be positive or negative; however, their signs are always opposite (see Fig. 3). This indicates that vibrational bands excited by E_{pt} and E_{pn} always appear inverted relative to each other. Second, ΔR_s is consistently negative, meaning that vibrational bands excited by s-polarized light appear as negative features in absorbance, corresponding to an increase in reflectance. In general we can conclude that the component of the TDM of an adsorbate vibration perpendicular to the surface only couples to the E_{pn} component of the incident light, thus resulting in a negative signal in absorbance. In contrast, the component of the TDM parallel to the surface can couple either to the E_{pt}, or the s-polarized light, depending on the direction of this vibration and the direction of the incident light. And third, an incidence angle of approximately 80° to 85° is required in experiments to achieve optimal sensitivity.

In summary, the observed spectral features in polarized IRRAS originate from the interaction between the incident electric field and the molecular TDM components, both parallel and perpendicular to the surface (Fig. 3). The strength of this interaction depends on the projection of the TDM onto the electric field vector, which varies with polarization and angle of incidence. This directional coupling governs the intensity and shape of the observed bands. In cases where a discrete vibrational mode interacts with a substrate or electronic states, Fano interference leads to characteristic asymmetric or inverted line shapes (Fig. 4).

A joint study combining IRRAS experiments and DFT calculations demonstrated azimuth- and polarization-dependent observation of formate species after adsorbing formic acid on ZnO.[9] It was shown that formic acid deprotonates on the mixed-terminated ZnO($10\bar{1}0$) surface resulting in two different formate species. For IR light incident along the [$1\bar{2}10$] direction, one positive band at 1573 cm^{-1} (asymmetric (OCO) stretching vibration band: ν_{as}(OCO)) and one negative band at 1374 cm^{-1} (symmetric (OCO) stretching vibration band: ν_s(OCO)) were observed in p-polarized light, while only one negative band at 1577 cm^{-1} was detected with s-polarized light. The ν_{as}(OCO) for a bidentate should be observed with E_{pn} component. So, here Buchholz *et al.*[9] considered another adsorption geometry rather than the bidentate species as a positive band was seen for the ν_{as}(OCO) band with p-polarized light. DFT calculations confirmed that a quasi-bidentate formate species forms on ZnO($10\bar{1}0$) with the TDM of the ν_{as}(OCO) band oriented along the [0001] direction, which can couple to the E_{pt} component for light incident along the [0001] azimuth leading to a positive band in IR spectrum. Most importantly, the results demonstrated that the sign and intensity of the observed IR bands for different formate species depend strongly on the polarization and direction of the light incidence. The ν_{as}(OCO) of the bidentate formate was either excited by the p-polarized light component E_{pt} along the [$1\bar{2}10$] direction or by the s-polarized light E_s along the [0001] azimuth *via* coupling with the TDM of the ν_{as}(OCO) vibration oriented along the [$1\bar{2}10$] direction. The dipole moment of the ν_{as}(OCO) was oriented along the [0001] azimuth for the quasi-bidentate configuration and therefore, it interacts with both E_{pt} (positive sign in absorbance, negative sign in reflectance) and the s-polarized light incident along [$1\bar{2}10$] direction (negative sign in absorbance, positive sign in reflectance). The larger frequency splitting in quasi-bidentate configuration compared to the bidentate formate was attributed to the additional hydrogen bond to the surface oxygen ions.[9]

The interaction of formic acid was investigated on anatase (101) and rutile (110) surfaces of TiO_2 as an important semiconductor and photoactive catalyst.[1,8] On a rutile surface, formic acid dissociates to formate species and binds with one oxygen to the five fold coordinated titanium sites (Ti_{5c}) in a monodentate configuration, resulting in two positive IRRAS bands assigned to the symmetric and asymmetric (OCO)

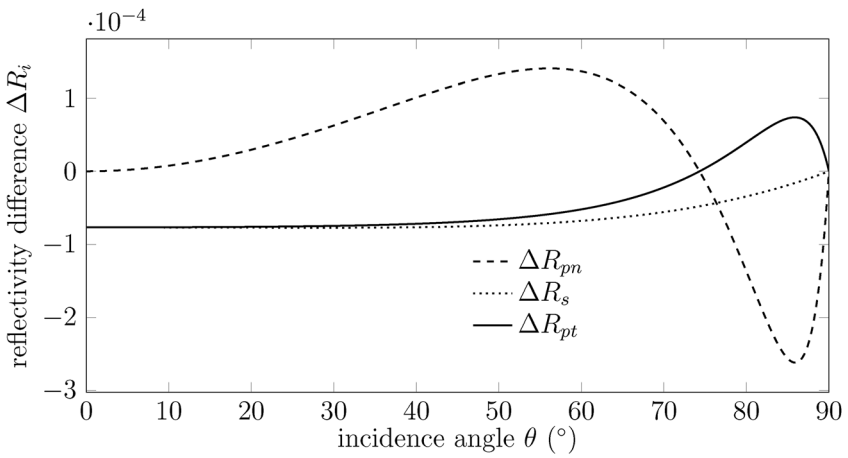

Fig. 3 Calculated reflectivity differences ΔR_s (dotted line), ΔR_{pt} (solid line) and ΔR_{pn} (dashed line) plotted as a function of the incidence angle θ for formic acid on magnetite. Calculation parameters: ν = 1380 cm^{-1}, n_1 = 1, k_1 = 0, n_2 = 1.37,[19] k_2 = 0.3, n_3 = 3.552, k_3 = 0, d_2 = 0.15 nm obtained from ref. 13 and 14.

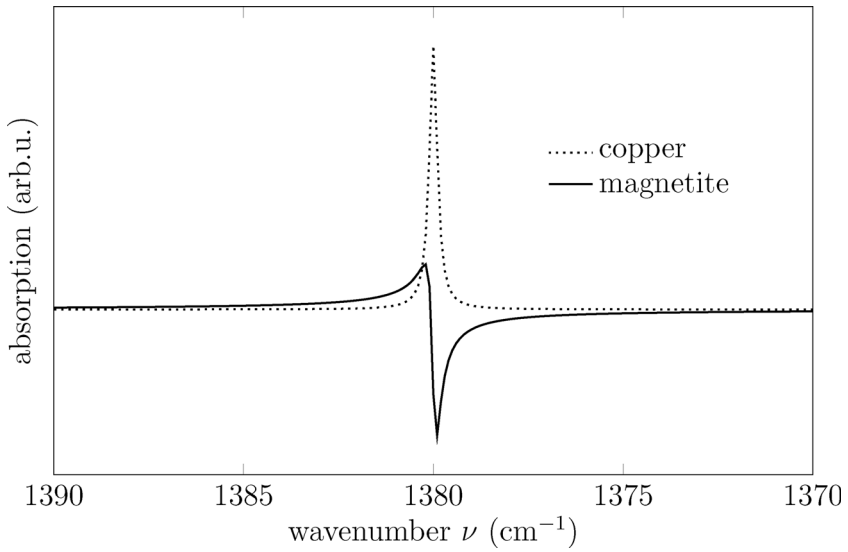

Fig. 4 Line shapes for a dynamic dipole perpendicular to the surface calculated at ν_0 = 1380 cm^{-1} and θ = 80° for magnetite (solid line) and copper (dashed line), demonstrating the reversal of the Fano line shape due to the change in TDM-field coupling. Other parameters used for the calculation: γ = 0.25 cm^{-1}, ε_3 = 10.924 + 9.242i obtained from ref. 13 and 14. The line shape for copper was calculated using Re(ε) = −2000 and Im(ε) = 400, which results in a symmetric line shape.[10]

stretching modes in the p-polarized IR spectrum. A bidentate formate configuration was further found to form *via* the interaction of both oxygen atoms in the carboxylate group of formate with Ti_{5c} sites. However, on reduced rutile TiO_2(110) a majority of bidentate formate was observed compared to the stoichiometric surface. In addition, the highly defective TiO_2(110) does not show any azimuth dependence, indicating a change in the adsorption geometries of formate species. This is probably due to an increase in the reduced Ti^{3+} cations formed during sputtering and an increase of the surface roughness.[18] Dissociative adsorption of HCOOH on an anatase (101) surface was further confirmed by a dominant negative feature around 1688 cm^{-1} associated with the (C═O) stretching vibration assigned to a monodentate formate species. The negative ν(C═O) band in both p- and s-polarized modes indicates that this bond of the adsorbed HCOOH is tilted from the surface normal and has components parallel and perpendicular to the surface.

Also, bidentate adsorption was confirmed in p-polarized spectra by negative IR bands of stretching vibrations for a symmetric (OCO) mode at 1361 cm^{-1}, a (HCO) mode at 1386 cm^{-1}, and the broad positive band of an asymmetric (OCO) mode at 1560 cm^{-1} (all signs are from the spectra plotted in absorbance). The sign of the absorbance feature for p-polarized light provided again crucial information on the orientation of the formate with respect to the surface normal. Negative absorbances for (C═O), symmetric (OCO) and (HCO) stretching vibrations are associated with their TDMs having components perpendicular to the surface. The positive absorbance for the asymmetric (OCO) stretching vibration shows the TDM orientation parallel to the surface in a bidentate configuration.[8,20]

The first IRRAS experiment of the adsorption of formic acid on a clean magnetite (001) surface[10] and following studies[11,21] demonstrated a unique feature of magnetite in IR spectroscopy that is known as Fano line shape. The Fano line shape[10] in IR spectroscopy can arise when there is an interaction between a discrete vibrational mode of an adsorbed molecule and a continuum of electronic or phononic states provided by the magnetite surface. Magnetite being neither a perfect metal nor a perfect insulator, presents IR bands that can be surprisingly seen by both s- and p-polarized light.

To illustrate this effect, Fig. 4 shows the spectral evolution from a symmetric absorption band to an asymmetric or inverted profile. This transition is governed by changes in the coupling strength between the vibrational mode and the electronic continuum, which may be influenced by factors such as surface reduction, adsorbate coverage, or substrate morphology. The expected line shape for a TDM oriented perpendicular to the surface is derived from the fractional change in reflectivity, as described in ref. 22. This approach was previously applied to interpret the IR line shapes observed during the dissociative adsorption of formic acid on magnetite.[10] The corresponding expression for the fractional change in reflectivity is:

$$\frac{\Delta R}{R} = \frac{I - I_0}{I_0} \sim -32\pi^2 \bar{\nu} \frac{\sin^2\theta}{\cos\theta} [\beta_1 \mathrm{Im}(N_s\alpha) + \beta_2 \mathrm{Re}(N_s\alpha)] \quad (1)$$

here $\bar{\nu}$ denotes the wavenumber. With:

$$\beta_1 = \mathrm{Re}\left[\frac{1}{\left(1-\frac{1}{\varepsilon_3}\right)\left(1-\frac{\tan^2\theta}{\varepsilon_3}\right)}\right] \text{ and}$$
$$\beta_2 = \mathrm{Im}\left[\frac{1}{\left(1-\frac{1}{\varepsilon_3}\right)\left(1-\frac{\tan^2\theta}{\varepsilon_3}\right)}\right]. \quad (2)$$

The polarizability of the adsorbate α is given by:

$$\alpha = \alpha_e + \frac{\alpha_v}{1 - \frac{v}{v_0}\left(\frac{v}{v_0} + i\frac{\gamma}{v_0}\right)} \quad (3)$$

Here, α_e represents the frequency-independent electronic polarizability, while α_v denotes the vibrational polarizability, with ν_0 as the resonant frequency and γ as the line width. The peak intensity is determined by the surface density of adsorbates N_s and the vibrational polarizability α_v. The complex dielectric function ε, related to the refractive index by $\varepsilon = \hat{n}^2$, also plays a key role.

Fig. 4 shows the calculated Fano line shape appeared at 1380 cm^{-1}, characteristic for a symmetric stretching vibration of ν_s(OCO) band, as we already expected and found in ref. 10. Here, we give an example on how the sign and the line shape of an IR band changes for an adsorbate on the surface of different substrates. Fig. 4 illustrates the calculated line shape of a dynamic dipole moment oriented perpendicular to the magnetite surface, with a resonance wavenumber of ν_0 = 1380 cm^{-1} and an incidence angle of $\theta = 80^\circ$. The resulting asymmetric Fano profile arises from the comparable real (n_3) and imaginary (k_3) parts of the refractive index ($n_3 \approx k_3$).[23] While variations in ν_0 affect the band amplitude, they leave the line shape unchanged. However, excitation by a different electric field component, such as E_{pt}, inverts the line shape due to the opposite sign of ΔR_{pt} relative to ΔR_{pn} (see Fig. 3). For copper, representing a typical metal, the line shape is calculated using Re(ε) = −2000 and Im(ε) = 400 (Fig. 4).[10,13] Due to the high dielectric constant of the metal substrate, changes in the fractional reflectivity arise solely from the adsorbate layer, leading to a symmetric line shape.[10,13]

The line shape of the vibrational band is, furthermore, very sensitive to the angle of incidence, θ. Fig. 5 shows the transition from an almost classical absorption line (red curve) to an inverted line shape (blue) in the range of the incident angles $70^\circ < \theta < 82^\circ$. The asymmetric Fano line shape band appears more pronounced in the angles around $74^\circ < \theta < 76^\circ$ which is exactly the range of incidence angle used in our experiments on magnetite samples in this study. The line shapes shown in Fig. 5 result from excitations with different components of the p-polarized electric field: E_{pt} and E_{pn}. When the excitation occurs *via* E_{pn}, the resulting spectral feature follows a Fano line shape (red curves). In contrast, excitation with E_{pt} produces an inverted line shape (blue curve), due to a sign change in the reflectivity difference ΔR_{pt}. This inversion arises because the IR line shape is sensitive to the relative orientation between the electric field vector and the TDM of the adsorbed species. Depending on whether the TDM is aligned more perpendicular or parallel to the surface, it couples more strongly to either E_{pn} or E_{pt}. The direction and magnitude of this coupling influence both the sign and intensity of the spectral response.

As a consequence, the observed line shape not only reflects the nature of the Fano resonance but also contains information about the geometry of the adsorbed molecules, specifically, whether they are oriented parallel or perpendicular to the surface. Fig. 5 illustrates how a change in field direction alters the sign of the TDM projection onto the field vector, thus inverting the Fano line shape. In this work, we show in detail how this plays a major role in analyzing and understanding the adsorption of formic acid on different surfaces of single-crystalline magnetite (111) and (001).

Experimental and computational methods

The experiments were performed in the UHV cluster of the DESY NanoLab.[24] The magnetite surface preparation of sputtering and annealing cycles took place in a UHV chamber (base pressure 1 × 10^{-10} mbar) equipped with an electron beam-assisted sample heating stage, gas inlets and a sputter gun. The interconnected UHV chambers linked by a tunnel, allowing sample transfer

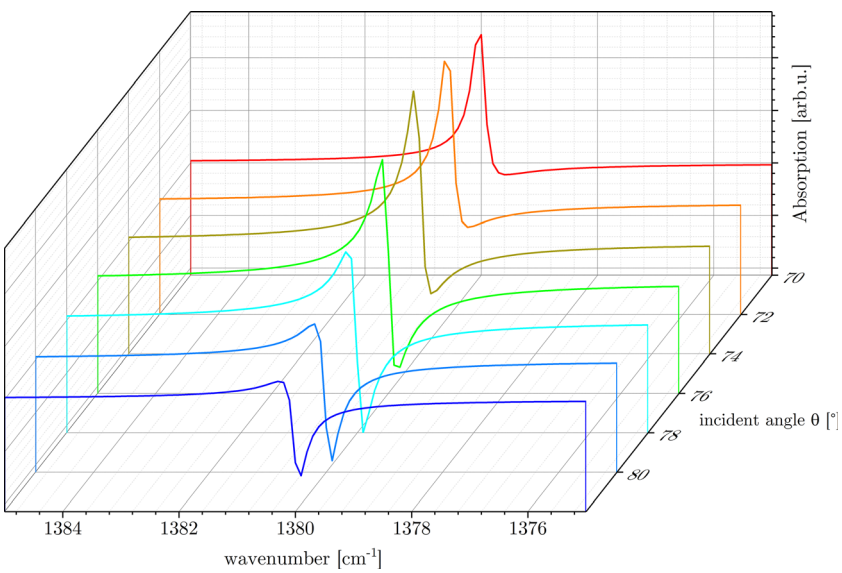

Fig. 5 Line shapes calculated around ν_0 = 1380 cm^{-1} for different incidence angles θ on magnetite. Parameters used: γ = 0.25 cm^{-1}, ε_3 = 10.924 + 9.242*i* obtained from ref. 13 and 14.

between the preparation and the IRRAS chambers without breaking ultra high vacuum. IRRAS measurements were performed at room temperature in a UHV system equipped with an IR spectrometer coupled to the UHV chamber *via* differentially pumped KBr-windows to avoid atmospheric moisture adsorption, thus resulting in a superior sensitivity and stability of the system. Each IR spectrum was accumulated in 1024 scans with a resolution of 2 cm^{-1} and was taken with the unpolarized and polarized beam at an incidence angle of 80° with respect to the surface normal at a base pressure of 4×10^{-10} mbar. The reflected signal was detected by a liquid nitrogen cooled mercury cadmium telluride (MCT) detector.

The IRRAS chamber is equipped with gas inlets and a resistive heater for sample temperatures up to 1000 K. The sample station can be cooled with liquid nitrogen to temperatures below 110 K. Both the optical bench of the spectrometer and the detector are evacuated to 2 mbar to reduce absorption from molecules like water, carbon monoxide, carbon dioxide and to ensure high sensitivity and long-term stability.

Prior to the IRRAS experiments, the surfaces of both Fe_3O_4(001) and Fe_3O_4(111) crystals were prepared using sputtering and annealing as it was reported in previous works[11,12,25,26] and were characterized using low-energy electron diffraction (LEED) and Auger electron spectroscopy (AES) to confirm the crystalline order, surface structure and surface purity.[24]

In our previous publications on formic acid adsorption at the two magnetite surfaces (001)[11] and (111),[12] dissociative adsorption was studied computationally in detail. Specifically, vibrational properties of adsorbates with binding modes where both carboxylate oxygens are bound to the surface, namely bidentate, quasi-bidentate and chelating, were calculated because of their high stability. Here, the vibrational properties for molecular and dissociative adsorption with a monodentate binding mode and a quasi-bidentate but *via* the restgroup hydrogen of formic acid were calculated at full coverage using density functional theory (DFT). To ensure comparability, the same computational setup as in our previous publications was employed here.

In short, spin-polarized DFT calculations were performed using the Vienna *Ab Initio* Simulation Package (VASP, version 5.4.4)[27–30] with the PBE + *U* approach[31,32] (U_{eff} = 4 eV on Fe d-electrons) and PAW pseudopotentials.[33] An energy cut-off of 520 eV and *k*-point grids of $7 \times 7 \times 1$ and $5 \times 5 \times 1$ for a 1×1 (111) and $\sqrt{2} \times \sqrt{2}$ R 45° (001) surface cell, respectively, allow for converged surface energies within 1 mJ m^{-2} and total energies within 3 meV per atom. Surfaces are modeled using symmetric periodic slabs with 13 and 17 layers for (001) and (111), respectively, separated by a vacuum region of about 23 Å. Vibrational frequencies and relative intensities are calculated in the harmonic approximation with Density Functional Perturbation Theory (DFPT) and using the Born Effective Charges (BEC).[34–39] Using this approach with the generalized gradient approximation (GGA) XC-functional PBE and the harmonic approximation introduces systematic errors. In the case of these two approximations, the errors often partially compensate for each other but the actual magnitude and direction of the overall error depends on the specific vibrational mode and the involved bonds. In the literature, an underestimation of the wavenumbers for vibrational modes, which include bonds between carbon and oxygen, has been observed compared to experimental results. The calculated wavenumbers often appear red-shifted in a range between 1% and 3.5%.[11,12,39–43] More details can be found in the SI.

The input VASP POSCAR files used for the DFT calculations in this work and for our previous studies[11,12] as well as a prototypical VASP INCAR file for calculating vibrational properties, particularly for adsorbates on magnetite surfaces, *via* DFPT can be found in the online repository TORE.[44] Additionally, xyz files containing atomic coordinate snapshots of calculated vibrational modes are available in this repository. Those xyz files allow to create animations of the vibrational modes using additional software such as Visual Molecular Dynamics (VMD).[45]

The additional DFT calculations were intended to be a proof of principle that certain adsorption types and modes give rise to vibrational bands in certain ranges. No extended adsorption structure search was however performed, and thus, effects of coverage, adsorbate superstructures, interactions between adsorbates with different adsorption types and modes, co-adsorption, and defects were not studied. The values for vibrational bands should therefore be considered as rough indicators only.

Results

According to our previous study[11] using unpolarized IR light, formic acid adsorbs dissociatively on the magnetite (001) surface at room temperature, resulting in a negative band at 1370 cm^{-1} and a positive band at 1538 cm^{-1} (both signs in absorbance), characteristic of the symmetric and asymmetric (OCO) stretching vibrations of formate species, respectively. Additionally, a positive band was observed at 1385 cm^{-1}, attributed to the CH bending mode, resulting also in an inverted Fano line shape, as compared to the symmetric stretching band. The adsorption of formic acid at 190 K led to another positive band at 1700 cm^{-1} on the magnetite (001) surface, assigned to the (C═O) stretching vibration of intact HCOOH molecules. DFT calculated vibrational bands for the adsorption of formic acid on two octahedral iron atoms with tetrahedrally coordinated Fe ions underneath (tet site) and interstitial sites underneath (int site) have further proven the experimental data regarding the (OCO) modes. The calculated vibrational frequency of the bidentate formate species on the interstitial site is found to slightly shift to lower wavenumbers.[11] It was, however, difficult to resolve the specific variations between the vibrational bands assigned to the tet and int sites in the experimental data because the s- and p-polarized beams could not be separated in the spectrometer and such separate measurements have not been performed earlier. A polarization-resolved IRRAS experiment, making use of the IR sign in polarized light, would therefore be crucial to unambiguously determine the adsorption geometries of the formate species and will be discussed in more detail later.

Similarly, formic acid adsorbs dissociatively on a Fe_3O_4(111) surface.[12,26] In the chelating adsorption geometry (1380 and 1548 cm^{-1}), both oxygen atoms of the carboxylate group are bound to one tetrahedral cation, while in the quasi-bidentate

adsorption geometry (1338 and 1588 cm^{-1}) one carboxylate oxygen atom binds to an iron tetrahedral site and the other to an OH group on the surface. No molecular adsorption or monodentate dissociation of formic acid was assumed due to an absence of the (C═O) vibrational band in the region 1600–1800 cm^{-1} in p-polarized light. The experimental and theoretical data confirmed that the distance between neighboring tetrahedral Fe atoms at the surface is 5.9 Å[12] and therefore, a bidentate bridging formate geometry was excluded, as this needs a shorter distance between the iron cations. Therefore, the IR bands at 1338 and 1588 cm^{-1} were assigned to a quasi-bidentate adsorption of formate. The other pair of symmetric (OCO) at 1380 cm^{-1} and asymmetric (OCO) at 1548 cm^{-1} with a smaller splitting was assigned to a chelating formate geometry as it presents a smaller (OCO) bond angle compared to a quasi-bidentate geometry on the magnetite (111) surface. The signs of the asymmetric (OCO) bands at 1548 and 1588 cm^{-1} are positive in absorbance mode of the IRRAS measured by p-polarized light, evidencing an excitation by the electric field component parallel to the surface, E_{pt}. The IR bands for symmetric (OCO) stretching vibrations are negative. This confirms that they originate from a TDM perpendicular to the surface or E_{pn}. Our experiments conducted by p-polarized IRRAS in combination with DFT calculations have shown that it is much easier to distinguish different adsorption bands assigned to the quasi-bidentate (1338 and 1588 cm^{-1}) and chelating (1380 and 1548 cm^{-1}) formate species[12] on Fe_3O_4(111) surface compared to all other oxide surfaces, because the corresponding IR bands are distinctly separated.

Since the line shape and sign of the IR bands provide the most promising information about the orientation of the adsorbed molecules and the electronic nature of the substrate, at the surface and interface, we will focus on this aspect in detail for the case study of adsorption of formic acid on single crystalline surfaces of magnetite (001) and (111) using IRRAS data obtained with both E_s and E_p-polarized light. To the best of our knowledge, such an analysis has not been reported before. Before presenting these IRRAS data, we first introduce our calculations regarding the expected signs and shapes of IR bands on magnetite surfaces.

The new IR spectra recorded in unpolarized beam, see Fig. 6a, show three bands at 1369, 1377 and 1385 cm^{-1} of which the first two bands belong to the symmetric stretching vibrations of (OCO) and the third to the C–H bending modes on Fe_3O_4(001). The vibrational stretching bands at 1538, 1515 and 1385 cm^{-1} are, however, all negative in the s-polarized spectra, see Fig. 6e, as a result of an increase in the reflectivity of the substrate at the position of the vibrational band. For the p-polarized spectra shown in Fig. 6c, the IR bands are much more intense and exhibit a Fano line shape, showing a different behavior compared to ZnO and TiO_2 surfaces.[8,9] In the spectra shown for the p-polarized beam all three bands observed earlier in the unpolarized light appear at higher frequency. We know that the line shape and sign in the p-polarized is different than in s-polarized light and depends on the incidence angle and the optical constant of the dielectric substrate.[7] As it was reported before by Yang *et al.*,[7] the position of the IR bands in the p-polarized beam is slightly higher than those observed at the s-polarized light. This observation was related to the discontinuity of the electric field component perpendicular to the surface, see ref. 7. The size of the shift was connected to the oscillator strength and the dielectric background. In the spectra of the unpolarized light, however, the second IR band at 1555 cm^{-1} (both in s- and p-polarized) and 1548 cm^{-1} (only in p-polarized), see Fig. 6c and e, was not identified in our previous work. We expect that the IR band at 1548 cm^{-1} is originated from a species adsorbed parallel to the Fe_3O_4(001) surface, such as adsorption at the edge of the steps, and further studies are needed to clarify this.

While all other IR bands are known from our previous work, the new bands at 1555 cm^{-1} (p-polarized) and 1538 cm^{-1} (s-polarized) need to be characterized. Because the band at 1555 cm^{-1} appears in both s-and p-polarized light, it might originate from a component parallel to the surface and it should be a formate species that interacts with the TDM parallel to the surface, resulting in an inverse line shape compared to its symmetric IR band below 1400 cm^{-1}. We assign this band also to the asymmetric stretching vibration of (OCO). In our previous work, based on the DFT calculations and surface X-ray diffraction results,[11] we reported two formate species in bidentate geometry on octahedrally coordinated Fe ions: one with a tetrahedral iron atom underneath and the other one with an interstitial iron sites underneath. However, we could not distinguish these two species in IR spectra obtained by unpolarized light. Using polarized light spectroscopy, we report the first observation of the asymmetric (OCO) stretching mode associated with an octahedrally coordinated Fe atom positioned above tetrahedrally coordinated Fe ions beneath the surface.[11] This vibrational feature appears at 1555 cm^{-1} and is clearly resolved from the lower-frequency band at 1548 cm^{-1}, which is attributed to an octahedral Fe site above an interstitial Fe atom. The negative symmetric stretching vibration at 1370 cm^{-1} in p-polarized light was a clear evidence that the TDM of this species interacts with E_{pn}. While the sign of asymmetric stretching vibration at 1548 cm^{-1} is positive due to the interaction of (OCO) vibration with the TDM parallel to the surface. Additionally, a negative band was observed in the s-polarized light at 1385 cm^{-1}, attributed to the CH bending mode, exhibits a TDM parallel to the surface, which is excited by the s-polarized and the E_{pt} polarized component parallel to the surface, resulting also in an inverted Fano line shape, as compared to the symmetric stretching band.

Additional DFT calculations were performed for molecular and dissociative adsorption of formic acid on magnetite (001) both with a monodentate binding mode where only one oxygen from the carboxyl group of the adsorbed formic acid is bound to a octahedral surface iron atom. These calculations suggest vibrational bands for the C═O stretching mode, of the oxygen bound to the surface, at around 1780 and 1660 cm^{-1} for molecular and dissociative adsorption, respectively. Since no bands are present in the experimental results at room temperature, such adsorption geometries can be ruled out here while they are plausible at low temperatures.

For the magnetite (111) surface the situation is even more complex. Here, as expected, the IR bands in the s-polarized

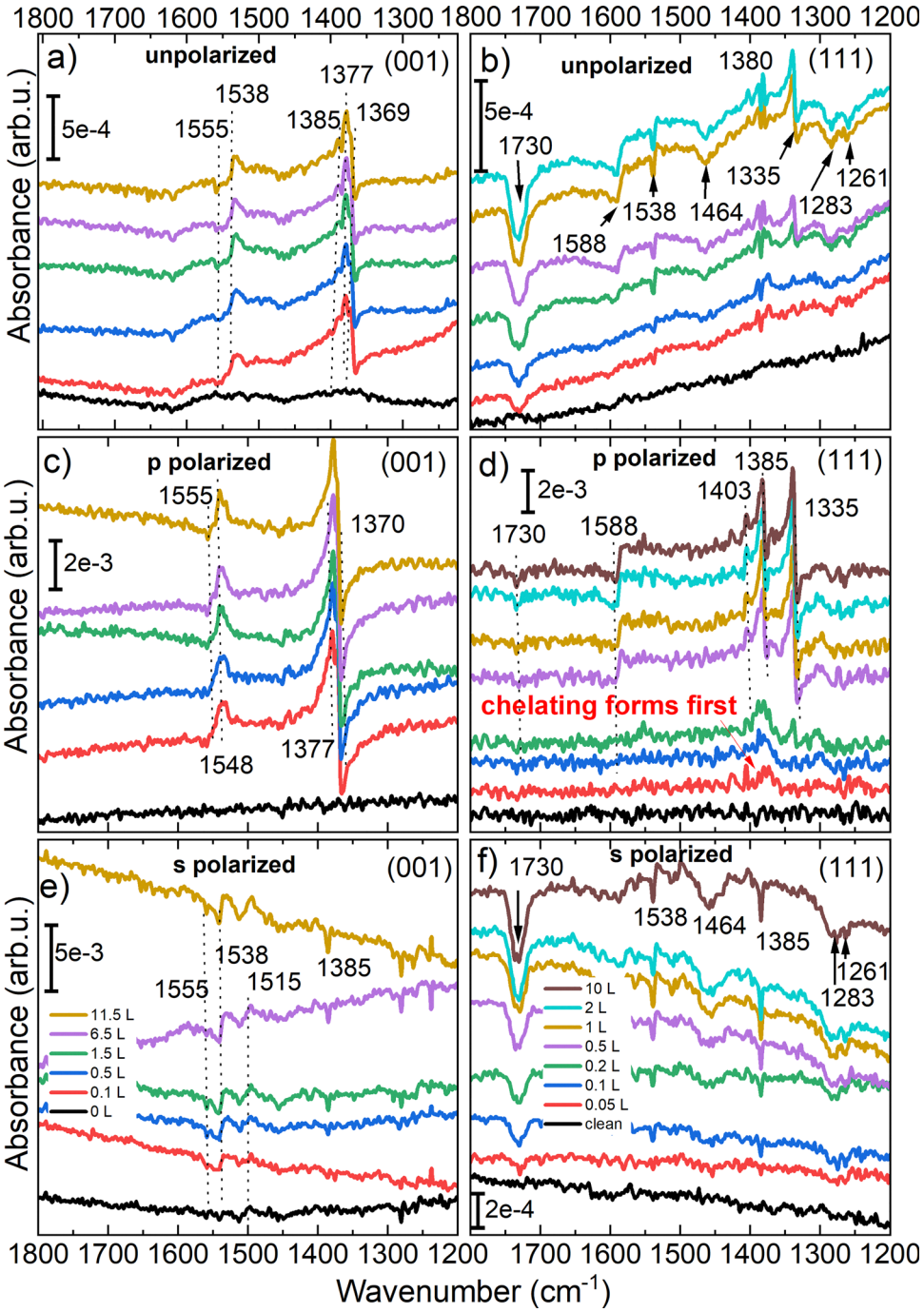

Fig. 6 Unpolarized, p-polarized and s-polarized FT-IR spectra in the region of carboxylic bands for different coverages of formic acid on magnetite (001) and (111) surfaces in the left and right column, respectively. The labels in Figure e and f denote the pressure during dosing, the dosing time, and the total exposure in Langmuir (1 L = 1.33 × 10^{-6} mbar s) for all spectra shown in unpolarized, s-polarized, and p-polarized light.

light are again all negative in absorbance. In the spectra shown in Fig. 6(b), (d) and (f), we observe dominant vibrational bands at 1335, 1380, 1538, 1588 and 1730 cm^{-1} after dosing formic acid on a magnetite (111) surface. The symmetric (OCO) stretching modes associated with quasi-bidentate and chelating geometries observed at 1335 and 1380 cm^{-1}, repectively, appear as negative signed Fano-type resonances in the unpolarized spectra. In contrast, the asymmetric (OCO) stretching vibration (1588 cm^{-1}) exhibits a positive (inverted) Fano line shape. Having a closer look on the coverage-dependent evolution of the spectra on magnetite (111) using a p-polarized beam, reveals that chelating formate forms first. A weak band is already visible at an exposure of 0.05 L (red curve in Fig. 6). The first evidence of the second adsorption geometry, quasi-bidentate, appears from a total exposure of 0.2 L (green curve). This is in line with our previous reports in ref. 12. The chelating adsorption geometry is

stabilized because atomic hydrogen from the dissociation of formate can go to the oxygen-terminated areas (around 20%). Once these O-terminated areas are covered by hydrogen, the quasi-bidentate geometry is more favorable (Table 1).

The observed vibrational bands are attributed to dissociated formic acid, consistent with the previous observations.[11,12] Molecular adsorption and monodentate formate formation were previously excluded due to the absence of the ν(C═O) vibrational band in the region between 1800–1600 cm^{-1}.[10] The IR spectra of the unpolarized and s-polarized light show an IR band at 1730 cm^{-1} which we did not observe before in the spectra of the p-polarized light reported in ref. 12 and 26. DFT calculations were carried out to evaluate the vibrational spectra of additional binding geometries not considered in our previous work,[12] which examined chelating and quasi-bidentate modes. Here, monodentate species and alternative quasi-bidentate species were considered for both molecular and dissociative adsorption of formic acid. The additionally calculated vibrational spectra, and the corresponding atomic coordinate input files can be found in the SI and the online repository TORE,[44] respectively, while detailed information on our previous calculations can be found in ref. 12 and 46.

In our previous work the hydrogen bond in the quasi-bidentate configuration was formed between the formate oxygen and a surface hydroxyl group whereas in the present case it is established *via* the hydrogen atom of the formic acid rest-group. For molecular adsorption the geometries are presented in Fig. 9, while the dissociated species show similar geometries only with the hydroxy hydrogen adsorbing to the surface. For molecular adsorption, indicative bands for stretching vibration of C═O at 1721 and 1649 cm^{-1} for monodentate and quasi-bidentate species, respectively, were suggested by DFT. In the case of dissociative adsorption those calculated bands are shifted to 1731 and 1585 cm^{-1} for monodentate and quasi-bidentate species, respectively. Both bands for quasi-bidentate species formed *via* the rest-group H of formic acid do not fit to the experimental results; therefore, the formation of such species is highly unlikely. The calculated bands for monodentate species are both close to the experimental values. Since the calculated bands using the described computational setup usually underestimate the experimental wavenumbers, molecular adsorption is more likely from the computational point of view but a definite conclusion cannot be made here. Thus, those IR band originate from a stretching vibration of C═O with the O bound to an Fe surface atom and therefore, we can propose that in addition to other chelating and quasi-bidentate (*via* the hydrogen in carboxyl group from the initial formic acid) geometries of formate species, some formic acid molecules adsorb either molecularly/undissociated or dissociatively yielding a monodentate species.

From the energetics such species are less stable than previously established chelating and quasi-bidentate geometries with adsorption energies of down to −2 eV per molecule. The adsorption energies are a factor of two to three smaller while the surface energies are about a factor of two larger. Even though no full adsorption structure search and optimization was performed here and thus this is no quantitative proof, these differences are a clear indication that such monodentate species are unlikely to be stable at clean surfaces. However, they might be formed as intermediates in the early stage of adsorption or if surface oxygens are already occupied, *e.g.*, by hydrogen atoms.

In the experiments, the band at 1730 cm^{-1} appears with high intensity in the s-polarized spectra, whereas it is significantly weaker in the p-polarized spectra. This observation indicates that the C═O group is not oriented completely parallel to the surface, but rather adopts a tilted configuration. Consequently, it can be excited by both E_{pn} and E_{pt} components with opposite signs, which leads to a partial cancellation of the signal in p-polarization. As a result, the band is observed predominantly in s-polarized light. This observation also argues against alternative quasi-bidentate species in which the C═O bond would lie more parallel to the surface, and instead supports monodentate geometries where the bond is more tilted.

The other new bands observed in the spectra of the unpolarized and the s-polarized lights are located at 1538, 1464, 1283 and 1261 cm^{-1}, which are nearly absent in the p-polarized light, giving a hint on originating from vibrations parallel to the surface. There are still three IR bands in the spectra of the unpolarized light at 1588, 1380 and 1335 cm^{-1}. The IR band at 1385 cm^{-1} has a positive sign in the p-polarized light and negative sign in the s-polarized light in adsorbance mode and is characteristic of the bending mode of the C–H vibration. The intensity of the band is high in the p-polarized light. Since the band can be observed in the s-polarized light with a negative sign and at higher frequency at 1385 cm^{-1}, we propose that the C–H bond is not completely perpendicular to the surface and is tilted or there are different C–H bands involved in the spectra of the s- and p-polarized lights, one from the dissociative molecule (formate species) and one from the non dissociated formic acid molecule (molecular adsorption). The IR band at 1335 cm^{-1} has a positive sign (down to up) in p-polarized light and is absent in the s- polarized light, while the IR band at 1588 cm^{-1} appears in both s- and p-polarized light with negative sing (up to down). The position of these bands are similar to the one reported for the quasi-bidentate adsorption of formate on ZnO(10$\bar{1}$0), (ν_s(OCO) at 1337 cm^{-1} and ν_{as}(OCO)

Table 1 Overview of experimental vibrational stretching (ν) and bending (δ) bands of formic acid adsorbed on magnetite (001) and (111)

Surface	Vibrational band	Wavenumber (cm^{-1})	Polarization
001	$\delta^{bb,tet}$(CH)	1373/1385	p$_t$/s
001	$\nu_s^{bb,int}$(OCO)	1377	p
001	$\nu_s^{bb,tet}$(OCO)	1369	p
001	—	1512	s
001	$\nu_{as}^{bb,int}$(OCO)	1548/1538	p/s
001	$\nu_{as}^{bb,tet}$(OCO)	1555	p
111	ν_s^{qbt}(OCO)	1335	p
111	ν_{as}^{qbt}(OCO)	1588	p
111	ν_s^{chel}(OCO)	1380	p
111	δ^{qbt}(CH)	1385	s
111	δ^{chel}(CH)	1280	s
111	—	1403	p
111	—	1464	s
111	ν_{as}^{chel}(OCO)	1548	p (very weak)
111	ν(CO)	1730	s

at 1589 cm^{-1}).[9] The smaller splitting of the ν_s(OCO) vibration at 1380 and ν_{as}(OCO) vibration at 1548 cm^{-1} is a result of a smaller (O–C–O) bond angle and a chelating adsorption geometry with both formate oxygen atoms bound to one single Fe_{tet1} ion.[47] The sign of IR bands demonstrates that the band at 1335 cm^{-1} is a ν_s(OCO) vibration of formate in a quasi-bidentate geometry with a line shape, down to up, originating from a dynamic field perpendicular to the surface E_{pn}, while the IR band at 1588 cm^{-1}, ν_{as}(OCO), is inverted, because it is excited by the electric field component parallel to the surface seen by E_s and E_{pt} components of the IR light.[11,18]

The IR band at 1464 cm^{-1} is observed in the unpolarized spectrum and exhibits a higher intensity in the s-polarized spectrum. Based on the literature, this band is attributed to adsorbed formic acid on solid surfaces; however, its assignment remains under discussion.

To obtain a quantitative analysis of the symmetric ν_s and asymmetric ν_{as} (OCO) stretching vibrations, the experimental IR spectra were fitted with theoretical line shapes based on eqn (1)–(3). Fig. 8 presents the fitted Fano profiles together with the experimental p-polarized spectra of the ν_s(OCO) and δ(CH) at 1372 cm^{-1}, see Table S8 of formate in the bidentate bridging configuration on magnetite (001). Notably, the δ(CH) mode exhibits an inverted Fano line shape. For magnetite (001), two distinct ν_{as}(OCO) Fano resonances of bidentate bridging formate at 1541 and 1552 cm^{-1}, see Table S8 are resolved. In contrast, for magnetite (111), the spectra are best described by two separate Fano components centered at approximately 1380 cm^{-1} and 1337 cm^{-1}, assigned to the ν_s(OCO) modes of formate in chelating and quasi-bidentate geometries, respectively. The fit parameters summarized in Fig. 8 and Table S8 (SI) further corroborate our vibrational assignments based on the sign of the Fano line shapes. Moreover, the fitting procedure independently confirms angles of incidence close to 75°.

Importantly, on the Fe_3O_4(111) surface, a new IR band appears at 1730 cm^{-1} in unpolarized and s-polarized light, in excellent agreement with DFT-predicted frequencies (1721 cm^{-1}) for a C═O stretching vibration. This feature is attributed to molecular formic acid adsorbed in a monodentate configuration. Its coexistence with formate species suggests a more complex adsorption landscape on the (111) surface, where both dissociative and molecular adsorption pathways occur.

The configuration in which formate binds to the surface influences both the symmetric and asymmetric (OCO) stretching frequency and the C–H vibrational frequencies. The C–H stretching vibrations of formate and formic acid on oxide surfaces tend to appear around 2800–3000 cm^{-1}. The exact position of these IR bands depends on the oxide, the coverage of the adsorbed species, and whether a molecular or dissociated form is present. The intensity of the C–H stretching bands is often much weaker than that of the symmetric and asymmetric (OCO) stretches, due to their smaller change in dipole moment.[48] This can be attributed to surface selection rules for IRRAS, the orientation and geometrical configuration of the adsorbate (molecular, bridging, monodentate, chelating, bidentate, *etc.*), the presence of defects, binding to under-coordinated atoms, and background contributions. All these, make the C–H stretch more difficult to observe. The number of studies that explicitly report the C–H stretching modes of adsorbed formate *via* IRRAS is small. A C–H stretching vibration around 2860 cm^{-1} was reported on NiO(111)/Ni(111) and assigned to either a bidentate or bridging formate configuration.[49] In one of the earliest detailed IRRAS studies, Hayden *et al.*[50] investigated the adsorption of formic acid on the Cu(110) surface. Upon deprotonation, formate species exhibited a clear C–H stretching vibration in the 2891–2900 cm^{-1} range, corresponding to the fundamental ν(CH) mode. Additionally, a combination band was observed near 2950 cm^{-1}, assigned to coupling of the asymmetric (OCO) stretch and the C–H bending vibrations.

In our study the polarization-resolved IRRAS measurements of the C–H stretching region reveal distinct differences in the adsorption geometries of formic acid on the Fe_3O_4(001) and Fe_3O_4(111) surfaces, see Fig. 7. On the Fe_3O_4(001) surface, four well-resolved C–H stretching bands were observed at 2848, 2868, 2917, and 2957 cm^{-1}. These bands exhibit clear polarization dependence: the bands at 2868 and 2957 cm^{-1} appear in p-polarized light, while those at 2848 and 2917 cm^{-1} are observed in s-polarized light. This polarization behavior indicates that the C–H dipole moments responsible for the 2848 and 2917 cm^{-1} bands are oriented parallel to the surface, while those of the 2868 and 2957 cm^{-1} bands have a significant in plane component. The IR band at 2957 cm^{-1} is, as previously reported, a coupling of the asymmetric (OCO) stretch and the C–H bending vibrations.[51] The 2868 cm^{-1} band, visible only in p-polarized light, strongly suggests an upright adsorption geometry, such as a bidentate formate species bound to octahedrally coordinated Fe atoms with tetrahedrally coordinated Fe ions underneath (tet). This interpretation is further supported by the observation of a strong asymmetric (OCO) stretching mode at 1555 cm^{-1}, also visible exclusively in p-polarized light. The alignment of both the C–H and (OCO) dipole moments perpendicular to the surface provides strong evidence for the presence of vertically oriented formate configuration.

The s-polarized 2848 and 2917 cm^{-1} bands likely correspond to more in-plane dipole moments, pointing to flatter configurations, probably to a bidentate formate adsorbed on interstitial sites (int).

The calculated spectra presented in the SI and in the literature[11,46] also include C–H stretching vibrations for the (001) surface. It has to be noted here, that the calculated wavenumbers should only be seen as rough indicators here because anharmonic effects, nuclear quantum effects[52–55] and ensemble effects[56] are likely to severely affect the spectra but were not properly accounted for neither in this study nor in the cited literature. All values presented in the following were obtained for half coverage defined by the ratio of adsorbates and Fe adsorption sites. For bidentate adsorption at the tet and int site the calculated wavenumbers for C–H stretching modes are 2943 and 2934 cm^{-1}, respectively. The C–H bond are perpendicular to the surface for both adsorption sites and should therefore produce a signal in p-polarized light. For monodentate adsorption, the calculated wavenumbers are 3065 and 3020 cm^{-1} for molecular and dissociative adsorption, respectively. The C–H bond for these monodentate species is tilted by about 70° *versus* the surface normal and should thus yield a

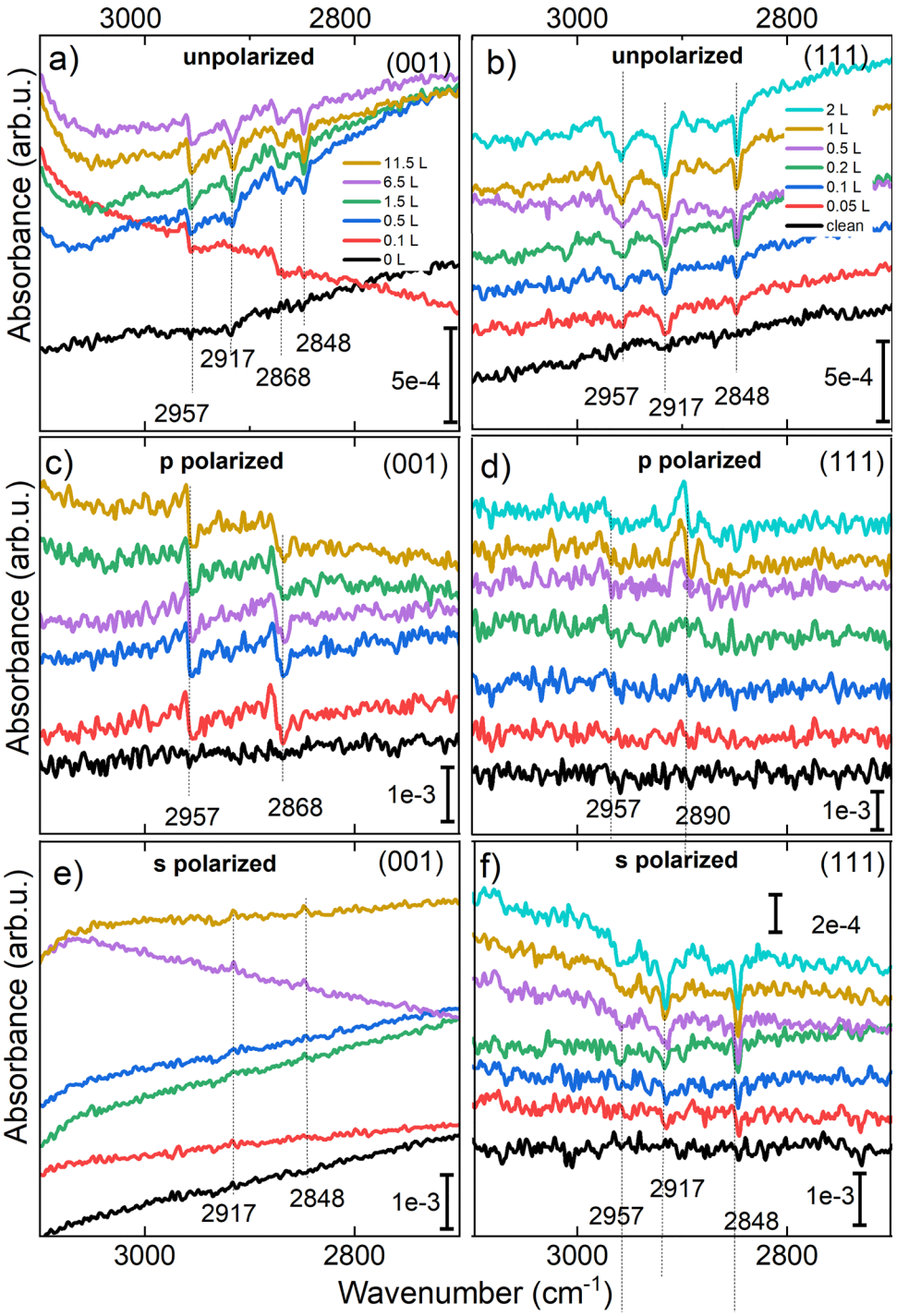

Fig. 7 Unpolarized and s- and p-polarized FT-IR spectra in the region of CH stretching bands for different coverages of formic acid on magnetite (001) and (111) surfaces in the top and bottom row, respectively. The labels in Figure a and b denote the pressure during dosing, the dosing time, and the total exposure in Langmuir (1L = 1.33 × 10^{-6} mbar s) for all spectra shown in unpolarized, s-polarized, and p-polarized light.

signal in s- and weakly in p-polarized light. The results fit to the experiments in general; however, a clear assignment is not possible because of the aforementioned reasons. For completeness, the wavenumbers of O–H stretching modes were obtained at around 3640 cm^{-1}. The O–H bonds were tilted *versus* the surface normal around 45° and 75° for surface hydroxy groups and within molecularly adsorbed formic acid, respectively.

In contrast, the Fe_3O_4(111) surface exhibits only three C–H stretching bands at 2848, 2917, and 2957 cm^{-1}, with the 2868 cm^{-1} band notably absent. The absence of the this band on the Fe_3O_4(111) surface and its presence on the Fe_3O_4(001) surface supports again different adsorption geometries, proving the polarization-resolved interpretation. All three bands appear in s-polarized light, with 2917 and 2957 cm^{-1} also present in

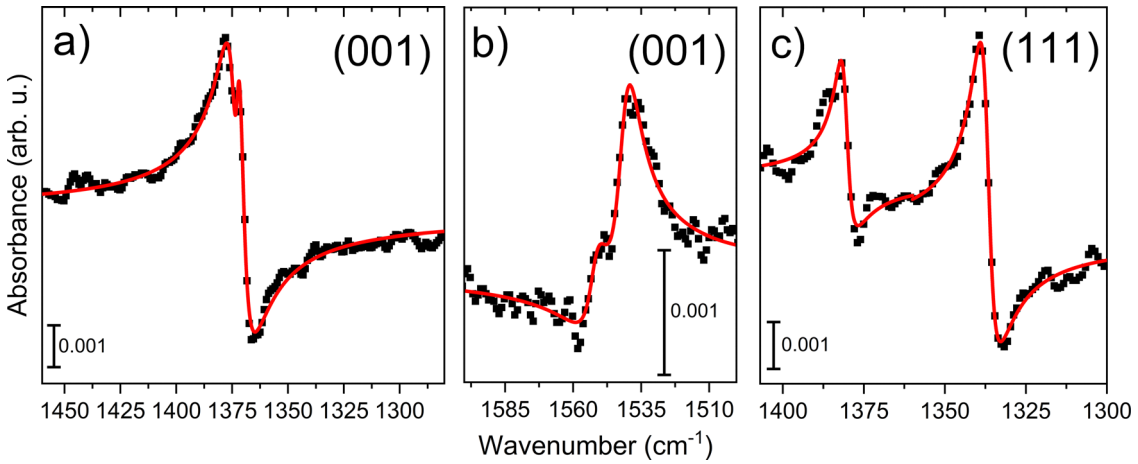

Fig. 8 Fitted vibrational Fano lineshapes (red lines) based on eqn (1)–(3) and experimental p-polarized data (black dots) of a) ν_s(OCO) and δ(CH) at 1372 cm^{-1} of formate in bidentate bridging geometry on magnetite (001). The line shape for δ(CH) is inverted. (b) Two ν_{as}(OCO) Fano lines of formate in bidentate bridging geometry on magnetite (001) at 1552 and 1541 cm^{-1}, see Table S8. (c) On magnetite (111), the data is fitted with two separate Fano lines around 1380 cm^{-1} and 1337 cm^{-1} of ν_s(OCO) of formate in chelating and quasi-bidentate geometry, respectively.

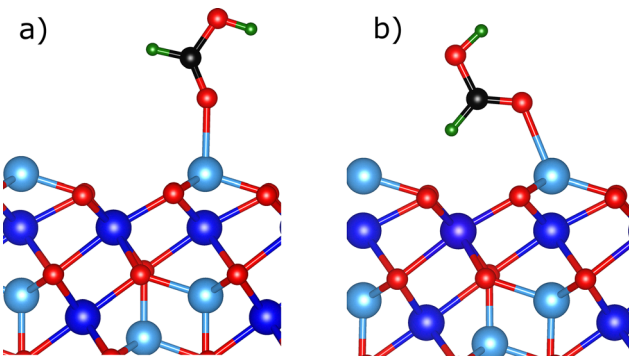

Fig. 9 Geometries for molecularly adsorbed formic acid on a tetrahedrally (tet1) terminated Fe_3O_4(111) surface. (a) Monodentate binding mode. (b) Quasi-bidentate binding mode.

p-polarized light, indicating primarily tilted or flat-lying adsorption geometries such as quasibidentate. The IR band at 2957 cm^{-1} is again a coupling of the asymmetric (OCO) stretch and the C–H bending vibrations.

The calculated spectra for the (111) surface provided in the SI and the literature[12,45] show various modes depending on the binding modes and the adsorption sites. Again, the wavenumbers have to be taken with care because of the limitations mentioned already for the (001) surface. Starting with dissociative adsorption where the C–H bonds are perpendicular to the surface, the C–H stretching modes for adsorbates in a chelating geometry were predicted at higher wavenumbers than for quasi-bidentate adsorbates. Chelating adsorbates at a low coverage of 1/3 of a monolayer (ML) gave rise to a C–H mode at 2959 cm^{-1}. Increasing the coverage to 1 ML, also shifted the wavenumber to higher values. Since those adsorbates were aligning in triangular clusters of three as evidenced in literature,[12] two different collective vibrational motions were observed. One was predicted at 2988 cm^{-1} with all C–H bonds stretching in phase. The other one was predicted at 2977 cm^{-1}, where a frustrated motions occurs, because a fully anti-phase motion is geometrically not possible but two adsorbates are in phase and the third shows an anti-phase motion. A fully parallel alignment of all adsorbates caused a shift of those wavenumbers by 2 cm^{-1}. Adsorbates in a quasi-bidentate geometry yielded C–H stretching modes depending on the adsorption site of the dissociated hydrogen. Adsorption with 1/3 ML coverage and the dissociated hydrogen placed at the first, second, and third nearest surface oxygen resulted in bands at 2935, 2919, and 2897 cm^{-1}, respectively. The C–H bonds were perpendicular to the surface for all of them. For adsorbates at 1 ML coverage exhibiting a monodentate binding mode, the C–H stretching wavenumbers were calculated to be 3060 and 3032 cm^{-1}, for molecular and dissociative adsorption, respectively. For those two cases, the C–H bonds were tilted *versus* the surface normal by about 75°. Interestingly, for the O–H stretching modes large deviations from the expected frequencies were observed. For vibrations of isolated surface hydroxyl groups or O–H groups in formic acid molecules, values around 3600 cm^{-1} were obtained, similar to the (001) surface. In contrast, for O–H modes of quasi-bidentate adsorbed formate species, the wavenumbers were strongly shifted and appeared to be highly sensitive to the specific adsorption geometry. For OH groups located at the first, second, and third nearest adsorption sites relative to the connected formate species, O–H stretching modes at 2944, 2651, and 2493 cm^{-1}, respectively, were predicted. In these cases, the O–H bonds were tilted by approximately 10 to 20°. However, the O–H bands on magnetite are intrinsically very weak and therefore not observable experimentally. Based on theoretical calculations, we can nevertheless confirm that dissociated hydrogen adsorbs on oxygen atoms of magnetite surfaces, leading to the formation of surface OH groups.

Taken together, these results highlight that the adsorption behavior of formic acid is strongly surface dependent. The (001) surface supports multiple formate species, including upright bidentate configurations with strong perpendicular dipoles, while the (111) surface favors flatter formates and monodentate

molecular species. The use of polarization-resolved IRRAS was essential in identifying these configurations and resolving overlapping bands that would remain ambiguous in unpolarized measurements. This work underscores the value of polarization-dependent spectroscopy in providing deeper insight into molecule–surface interactions, especially for complex oxide surfaces.

Conclusions

We performed Infrared Reflection Absorption Spectroscopy (IRRAS) studies in both s- and p-polarized light, along with DFT calculations, to investigate the adsorption of formic acid on Fe_3O_4(001) and Fe_3O_4(111) single-crystal surfaces. By analyzing the spectra of both s- and p-polarized light and comparing them with the spectra of unpolarized light as well as with calculated vibrational spectra, we obtained new insight into the geometry and adsorption type of the species, including several new adsorbed configurations that were not observed in previous measurements with unpolarized IR light. Our results explore more adsorption geometries than previously reported and show the importance of polarized light studies on oxide surfaces.

On the magnetite (001) surface, we found a new band at 1555 cm^{-1} in p-polarized light. Because it is seen only in p-polarized light and is absent in s-polarized light, we excluded a vibration parallel to the surface and assigned it to a formate species that interacts with the TDM perpendicular to the surface. This is our first and direct experimental evidence of the asymmetric stretching vibration of (OCO) of a bidentate formate on octahedrally coordinated Fe ions with a Fe-tet underneath on this surface.

In addition to the chelating and quasi-bidentate formate geometries on the magnetite (111) surface, we observed a new IR band at 1730 cm^{-1} in both unpolarized and s-polarized light and in good agreement with DFT calculations (1721 cm^{-1}) originating from a stretching vibration of C═O. Therefore, we conclude that formic acid also shows a monodentate geometry in addition to formate species in chelating and quasi-bidentate geometries on magnetite (111) surface.

Furthermore, we reported the first C–H stretching bands for the adsorption of formic acid on magnetite surfaces sensitive to both s- and p-polarized light, confirming distinct adsorption geometries of formate on the Fe_3O_4(001) and Fe_3O_4(111) surfaces.

The experimental polarization-resolved IRRAS data provide direct evidence that not only the adsorption sites of the magnetite (111) and (001) are different, but the adsorption behavior of formic acid on these surfaces also varies. Taken together, these results highlight that the adsorption behavior of formic acid is strongly surface-orientation dependent.

Our observations demonstrate that by analyzing the positive and negative lines of IR bands, we can infer molecular behavior, adsorption and chemical transformations of molecules at the surface of adsorbates. We note that the polarization-dependent effects in IRRAS data on oxide surfaces may have a more complex nature, as described in recent work.[57] Overall, our work provides a powerful approach for investigating the interface between a molecule and an oxide surface, including the adsorption, molecular orientation, and bonding nature of formic acid in various environments.

Author contributions

H.N.: conceptualization, analysis of all FT-IRRAS data, manuscript writing and editing, supervision, funding acquisition; M.C.: sample preparation, FT-IRRAS experiments, G.V-F.: Conceptualization and execution of DFT calculations, analysis of data, funding acquisition, manuscript writing; A.S.: conceptualization, manuscript editing.

Conflicts of interest

There are no conflicts to declare.

Data availability

The data supporting the findings of this study are available within the article. Additional datasets generated and analyzed during the current study are available from the corresponding author upon reasonable request. Input files (POSCARs and a prototypical INCAR) of the DFT calculations and xyz files containing atomic coordinate snapshots of calculated vibrational modes are available at the online repository TUHH Open Research (TORE), DOI: https://doi.org/10.15480/882.15191.

The supplementary information (SI) provides a discussion of the accuracy of the calculated vibrational wavenumbers and contains plots and tabulated data of the calculated IR spectra and fit parameters for selected Fano lines from the experimental spectra. See DOI: https://doi.org/10.1039/d5cp00848d.

Acknowledgements

The authors thank Kai Sellschopp for his valuable input, as well as him and Francesca Schulze for their support in setting up the data repository at TORE. This project is funded by the Deutsche Forschungsgemeinschaft (DFG, German Research Foundation) – Projektnummer 192346071–SFB 986. We acknowledge DESY (Hamburg, Germany), a member of the Helmholtz Association HGF, for the provision of experimental facilities.

References

1 B. E. Hayden, in *Vibrational Spectroscopy of Molecules on Surfaces*, ed. J. T. Yates and T. E. Madey, Springer, 1987, vol. 1, pp. 267–344.
2 G. Rupprechter, *Annu. Rep. Prog. Chem., Sect. C: Phys. Chem.*, 2004, **100**, 237–311.
3 P. R. Griffiths and J. A. de Haseth, *Fourier Transform Infrared Spectrometry*, John Wiley & Sons, Ltd, 2nd edn, 2006.
4 Y. Wang, A. Glenz, M. Muhler and C. Wöll, *Rev. Sci. Instrum.*, 2009, **80**, 113108.
5 H. Noei, H. Qiu, Y. Wang, E. Löffler, C. Wöll and M. Muhler, *Phys. Chem. Chem. Phys.*, 2008, **10**, 7092–7097.

6 H. Noei, F. Gallino, L. Jin, J. Zhao, C. Di Valentin and Y. Wang, *Angew. Chem., Int. Ed.*, 2013, **52**, 1977–1981.
7 C. Yang, W. Wang, A. Nefedov, Y. Wang, T. G. Mayerhöfer and C. Wöll, *Phys. Chem. Chem. Phys.*, 2020, **22**, 17129–17133.
8 M. Xu, H. Noei, M. Buchholz, M. Muhler, C. Wöll and Y. Wang, *Catal. Today*, 2012, **182**, 12–15.
9 M. Buchholz, Q. Li, H. Noei, A. Nefedov, Y. Wang, M. Muhler, K. Fink and C. Wöll, *Top. Catal.*, 2015, **58**, 174–183.
10 O. Gamba, H. Noei, J. Pavelec, R. Bliem, M. Schmid, U. Diebold, A. Stierle and G. S. Parkinson, *J. Phys. Chem. C*, 2015, **119**, 20459–20465.
11 B. Arndt, K. Sellschopp, M. Creutzburg, E. Grånäs, K. Krausert, V. Vonk, S. Müller, H. Noei, G. Vonbun-Feldbauer and A. Stierle, *Commun. Chem.*, 2019, **2**, 92.
12 M. Creutzburg, K. Sellschopp, S. Tober, E. Granas, V. Vonk, W. Mayr-Schmölzer, S. Muller, H. Noei, G. B. Vonbun-Feldbauer and A. Stierle, *J. Phys. Chem. Lett.*, 2021, **12**, 3847–3852.
13 M. Querry, Contractor Report CRDC-CR-85034, 1985.
14 A. Schlegel, S. Alvarado and P. Wachter, *J. Phys. C-Solid State Phys.*, 1979, **12**, 1157–1164.
15 W. N. Hansen, *J. Opt. Soc. Am.*, 1968, **58**, 380–390.
16 W. N. Hansen, *Symp. Faraday Soc.*, 1970, **4**, 27–35.
17 J. A. Mielczarski and R. H. Yoon, *J. Phys. Chem.*, 1989, **93**, 2034–2038.
18 Y. Wang and C. Wöll, *Chem. Soc. Rev.*, 2017, **46**, 1875–1932.
19 C. Wohlfarth, *Optical Constants: Supplement to Volume III/47*, Springer, 2017, https://materials.springer.com/bp/docs/978-3-662-49236-9.
20 C. Yang, M. Capdevila-Cortada, C. Dong, Y. Zhou, J. Wang, X. Yu, A. Nefedov, S. Heißler, N. López and W. Shen, *et al.*, *J. Phys. Chem. Lett.*, 2020, **11**, 7925–7931.
21 D. Rath, V. Mikerásek, C. Wang, M. Eder, M. Schmid, U. Diebold, G. S. Parkinson and J. Pavelec, *Rev. Sci. Instrum.*, 2024, **95**, 065106.
22 R. G. Tobin, *Phys. Rev. B:Condens. Matter Mater. Phys.*, 1992, **45**, 12110–12113.
23 A. E. Miroshnichenko, S. Flach and Y. S. Kivshar, *Rev. Mod. Phys.*, 2010, **82**, 2257–2298.
24 A. Stierle, H. Noei, T. F. Keller, V. Vonk and R. Röhlsberger, *JLSRF*, 2016, **2**, A76.
25 B. Arndt, M. Creutzburg, E. Grånäs, S. Volkov, K. Krausert, A. Vlad, H. Noei and A. Stierle, *J. Phys. Chem. C*, 2019, **123**, 26662–26672.
26 M. Creutzburg, K. Sellschopp, R. Gleißner, B. Arndt, G. B. Vonbun-Feldbauer, V. Vonk, H. Noei and A. Stierle, *J. Phys.: Condens. Matter*, 2022, **34**, 164003.
27 G. Kresse and J. Furthmuller, *Comput. Mater. Sci.*, 1996, **6**, 15–50.
28 G. Kresse and J. Furthmuller, *Phys. Rev. B:Condens. Matter Mater. Phys.*, 1996, **54**, 11169–11186.
29 G. Kresse and J. Hafner, *Phys. Rev. B:Condens. Matter Mater. Phys.*, 1993, **47**, 558–561.
30 G. Kresse and J. Hafner, *Phys. Rev. B:Condens. Matter Mater. Phys.*, 1994, **49**, 14251–14269.
31 J. P. Perdew, K. Burke and M. Ernzerhof, *Phys. Rev. Lett.*, 1996, **77**, 3865–3868.
32 S. L. Dudarev, G. A. Botton, S. Y. Savrasov, C. J. Humphreys and A. P. Sutton, *Phys. Rev. B:Condens. Matter Mater. Phys.*, 1998, **57**, 1505–1509.
33 P. E. Blöchl, *Phys. Rev. B:Condens. Matter Mater. Phys.*, 1994, **50**, 17953–17979.
34 S. Baroni, P. Giannozzi and A. Testa, *Phys. Rev. Lett.*, 1987, **58**, 1861–1864.
35 P. Giannozzi and S. Baroni, *J. Chem. Phys.*, 1994, **100**, 8537–8539.
36 X. Gonze, *Phys. Rev. A:At., Mol., Opt. Phys.*, 1995, **52**, 1086–1095.
37 P. Giannozzi and S. Baroni, *Handbook of Materials Modeling*, Springer, Dordrecht, 2005, pp. 195–214.
38 D. Karhanek, T. Bucko and J. Hafner, *J. Phys.: Condens. Matter*, 2010, **22**, 265006.
39 T. Würger, W. Heckel, K. Sellschopp, S. Müller, A. Stierle, Y. Wang, H. Noei and G. Feldbauer, *J. Phys. Chem. C*, 2018, **122**(34), 19481–19490.
40 D. Porezag and M. R. Pederson, *Phys. Rev. B:Condens. Matter Mater. Phys.*, 1996, **54**, 7830–7836.
41 I. M. Alecu, J. Zheng, Y. Zhao and D. G. Truhlar, *J. Chem. Theory Comput.*, 2010, **6**, 2872–2887.
42 E. S. Skibinski, W. J. I. DeBenedetti and M. A. Hines, *J. Phys. Chem. C*, 2017, **121**, 14213–14221.
43 X. Li, J. Paier, J. Sauer, F. Mirabella, E. Zaki, F. Ivars-Barcelo, S. Shaikhutdinov and H.-J. Freund, *J. Phys. Chem. B*, 2017, **122**, 527–533.
44 G. Vonbun-Feldbauer and K. Sellschopp, Data for Computational vibrational spectra for formic acid adsorbed on magnetite surfaces from DFT calculations, TUHH Open Research (TORE) Repository, DOI: 10.15480/882.15191, 2025, https://tore.tuhh.de/handle/11420/55635.
45 W. Humphrey, A. Dalke and K. Schulten, *J. Mol. Graph.*, 1996, **14**, 33–38.
46 K. Sellschopp, PhD thesis, TU Hamburg, Germany, 2021.
47 M. Nara, H. Torii and M. Tasumi, *J. Phys. Chem.*, 1996, **100**, 19812–19817.
48 A. Mattsson, S. Hu, K. Hermansson and L. Osterlund, *J. Chem. Phys.*, 2014, **140**, 034705.
49 J. Kubota, T. Ohtani, A. Wada, J. N. Kondo, K. Domen and C. Hirose, *J. Phys. Chem.*, 1996, **100**, 14666–14672.
50 B. E. Hayden, K. Prince, D. P. Woodruff and A. M. Bradshaw, *Surf. Sci.*, 1983, **133**, 589–602.
51 J. Harris, S. Andersson and B. N. J. Persson, *Phys. Rev. Lett.*, 1983, **51**, 475–478.
52 M. Rossi, P. Gasparotto and M. Ceriotti, *Phys. Rev. Lett.*, 2016, **117**, 115702.
53 M. Rossi, *J. Chem. Phys.*, 2021, **154**, 170902.
54 G. Tabacchi, M. Fabbiani, L. Mino, G. Martra and E. Fois, *Angew. Chem., Int. Ed.*, 2019, **58**, 12431–12434.
55 E. Fallacara, F. Finocchi, M. Cazzaniga, S. Chenot, S. Stankic and M. Ceotto, *Angew. Chem., Int. Ed.*, 2024, **63**, e202409523.
56 A. Kotobi, L. Schwob, G. B. Vonbun-Feldbauer, M. Rossi, P. Gasparotto, C. Feiler, G. Berden, J. Oomens, B. Oostenrijk, D. Scuderi, S. Bari and R. H. Meibner, *Commun. Chem.*, 2023, **6**, 46.
57 B. Zerulla, M. Krstic, S. Chen, Z. Yu, D. Beutel, C. Holzer, M. Nyman, A. Nefedov, Y. Wang and T. G. Mayerhöfer, *et al.*, *Phys. Chem. Chem. Phys.*, 2024, **26**, 13683–13693.

